Energy dependent growth of nucleon and inclusive charged hadron distributions *

WANG Hong-Min(王宏民)[1] HOU Zhao-Yu(侯召宇)[2;1)] SUN Xian-Jing(孙献静)[3]

[1] Physics Department, Academy of Armored Forces Engineering of PLA, Beijing 100072, China
[2] Physics Graduate School, Shijiazhuang Railway Institute, Shijiazhuang 050043, China
[3] Institute of High Energy Physics, Chinese Academy of Sciences, Beijing 100049, China

Abstract: In the Color Glass Condensate formalism, charged hadron p_{T} spectra in p+p and p+Pb collisions are studied by considering an energy-dependent broadening of nucleon density distribution. Then, in the glasma flux tube picture, the n-particle multiplicity distributions at different pseudo-rapidity ranges are investigated. Both the theoretical results show good agreement with the recent experimental data from ALICE and CMS at LHC energies. The predictive results for p_{T} or multiplicity distributions in p+p and p+Pb collisions at the Large Hadron Collider are also given in this paper.

Key words: charged hadron p_{T} distributions, glasma flux tube, gluon saturation model

PACS: 25.75.-q, 24.85.+p, 14.20.Dh **DOI:** 10.1088/1674-1137/39/11/114105

1 Introduction

The measurement of the charged hadron transverse momentum (p_{T}) spectrum in heavy-ion collisions is a very significant topic in experimental physics. Recently, the ALICE and CMS experiments at the Large Hadron Collider (LHC) gave data for charged hadron p_{T} distributions in p+p collisions at $\sqrt{s}$=0.9, 2.36, 7 TeV [1, 2]. The experimental results show that the scaling features of charged hadrons previously observed at lower energies do not hold good at high energies. These indicate that we still do not have a basic understanding of the mechanism involved in charged particle production. Thus, a systematic theoretical study on this topic is still very necessary.

An effective theory to study the charged hadron p_{T} spectrum is the Color Glass Condensate (CGC) approach [3]. The CGC is a state predicted by quantum chromodynamics (QCD) at high energies where gluons in a hadron wave function are expected to condense. The cornerstone of the CGC approach is the existence of a hadron saturation scale Q_{s} at which gluon recombination effects start to balance gluon radiation. In order to give an accurate theoretical analysis, the nucleon density distribution in position space must be considered. Thus, the saturation scale Q_{s} should be considered as a function of the nucleon thickness function, $T_{\mathrm{p}}(b)$. Furthermore, due to gluon saturation, the width of the gluon distribution inside a nucleon should grow with collision energy $\sqrt{s}$ [4]. This will lead to a broadening of the nucleon density distribution in position space as $\sqrt{s}$ increases. Therefore, an energy-dependent broadening of the nucleon thickness function in the Q_{s} should also be considered.

Based on the CGC theory, many phenomenological saturation models, such as the Golec-Biernat and Wüsthoff (GBW) model [5], the Kharzeev, Levin and Nardi (KLN) model [6], the CGC model [7] and the Kovchegov, Lu and Rezaeian (KLR) model [8] have been proposed. It should be noted that the KLR model is based on the anti-de Sitter space/conformal field theory (AdS/CFT). In this paper, the KLN model and the KLR-AdS/CFT model are used because the simple analytic unintegrated gluon distribution functions can be obtained by a Fourier transform from the dipole amplitude of these two models.

Integrating charged hadron transverse momentum distributions over $\boldsymbol{p}_{\mathrm{T}}$, we can obtain the impact parameter ($\boldsymbol{b}$) dependent mean multiplicity, $\bar{n}(\boldsymbol{b})$. The mean multiplicity and the parameter controlling the size of the fluctuations, k, are two parameters that characterize a negative binominal distribution (NBD) [9, 10]. In the CGC picture, particles produced locally in the transverse plane are considered as correlated by approximately boost-invariant flux tubes [11]. Since there are $Q_{\mathrm{s}}^2 S_{\perp}$ such flux tubes emitting gluons, the parameter k should be proportional to $Q_{\mathrm{s}}^2 S_{\perp}$, where $S_{\perp}$ is the transv-

Received 8 January 2015, Revised 3 June 2015
* Supported by Natural Science Foundation of Hebei Province (A2012210043)
1) E-mail: houzhaoyu@stdu.edu.cn; whmw@sina.com.cn

erse overlap area of two collision hadrons. This indicates that the parameter k in the NBD is also a function of the thickness function, $T_{\rm p}(b)$, and influenced by the energy-dependent broadening. By convolving the NBD and the probability for an inelastic collision over the impact parameter, the n-particle multiplicity distributions can be obtained.

2 Energy dependent growth of nucleon and charged hadron $p_{\rm T}$ distributions

In hadron-hadron collisions, the transverse momentum distributions for gluons at leading order can be expressed as [12]

$$\begin{aligned}\frac{{\rm d}N_{\rm g}(\boldsymbol{b})}{{\rm d}^2\boldsymbol{p}_{\rm T}} = & \frac{1}{C_{\rm F}}\frac{1}{p_{\rm T}^2}\int{\rm d}y\int{\rm d}^2\boldsymbol{r}_{\rm T}\int_0^{p_{\rm T}}{\rm d}^2\boldsymbol{k}_{\rm T}\alpha_{\rm s}(Q^2)\\ & \times\phi_1\left(x_1,\frac{(\boldsymbol{k}_{\rm T}+\boldsymbol{p}_{\rm T})^2}{4},\boldsymbol{b}\right)\\ & \times\phi_2\left(x_2,\frac{(\boldsymbol{k}_{\rm T}-\boldsymbol{p}_{\rm T})^2}{4},\boldsymbol{b}-\boldsymbol{r}_{\perp}\right),\end{aligned} \quad (1)$$

where $N_{\rm c}=3$, $x_{1,2}=(p_{\rm T}/\sqrt{s})\exp(\pm y)$, and $C_{\rm F}=(N_{\rm c}^2-1)/(2\pi^3N_{\rm c})$. The running coupling constant

$$\alpha_{\rm s}(Q^2)=\min\left\{\frac{4\pi}{9\ln[Q^2/\Lambda_{\rm QCD}^2]},0.5\right\}$$

with $\Lambda_{\rm QCD}=0.2$ GeV and $Q^2=\max\{(\boldsymbol{k}_{\rm T}+\boldsymbol{p}_{\rm T})^2)/4,(\boldsymbol{k}_{\rm T}-\boldsymbol{p}_{\rm T})^2)/4\}$. $\boldsymbol{b}$ and $\boldsymbol{r}_{\perp}$ are the impact factor and the transverse position of the gluon, respectively.

In Eq. (1), ϕ is the unintegrated gluon distribution (UGD). In the KLN model, ϕ can be taken as [6]

$$\phi(x,k^2,\boldsymbol{b})=\frac{\xi C_{\rm F}Q_{\rm s}^2}{\alpha_{\rm s}(Q_{\rm s}^2)}\begin{cases}\dfrac{1}{Q_{\rm s}^2+\Lambda^2}, & k\leqslant Q_{\rm s}\\ \dfrac{1}{k^2+\Lambda^2}, & k>Q_{\rm s}\end{cases}, \quad (2)$$

where ξ is a normalization factor, and the saturation scale [4, 5]

$$Q_{\rm s}^2(x)=Q_0^2\left(\frac{0.01}{x}\right)^{\lambda}, \quad (3)$$

where $Q_0^2=2$ GeV^2, $\lambda=0.288$. In the KLR-AdS/CFT model, ϕ can be obtained by a Fourier transform from the dipole-nucleus amplitude given in Ref. [8]

$$\begin{aligned}\phi^{\rm AdS}(x,k^2,\boldsymbol{b}) = & \int{\rm d}^2\boldsymbol{r}{\rm e}^{{\rm i}\boldsymbol{k}\cdot\boldsymbol{r}}N(x,r)\\ = & \frac{32\pi}{(Q_{\rm s}^{\rm AdS})^2}\frac{1}{[1+16k^2/(Q_{\rm s}^{\rm AdS})^2]^{3/2}},\end{aligned} \quad (4)$$

where the corresponding saturation scale

$$Q_{\rm s}^{\rm AdS}(x)=\frac{2A_0x}{M_0^2(1-x)\pi}\left(\frac{1}{\rho_{\rm m}^3}+\frac{2}{\rho_{\rm m}}-2M_0\sqrt{\frac{1-x}{x}}\right). \quad (5)$$

The parameters $\rho_{\rm m},M_0$ and A_0 in Eq. (5), as given in Ref. [8], can be obtained by a fit to HERA data.

In order to give an accurate theoretical analysis, the UGD should be considered as a function of the transverse position distribution of the nucleon. Thus, the gluon saturation momentum is always written as [4]

$$Q_{\rm s,p(A)}^2(x,\boldsymbol{b})=Q_{\rm s}^2(x)\left(\frac{T_{\rm p(A)}(\boldsymbol{b})}{T_{\rm p(A),0}}\right), \quad (6)$$

where the nuclear thickness function

$$T_{\rm p(A)}(\boldsymbol{b})=\int{\rm d}z\rho_{\rm p(A)}(\boldsymbol{b},z),$$

and $T_{\rm p(A),0}=1.53$ fm^{-2} [4]. For the nuclear density distribution, we use the Woods-Saxon form [13]

$$\rho_{\rm A}(\boldsymbol{b},z)=\frac{\rho_0}{1+\exp[(r-R)/a]}, \quad (7)$$

where $r=\sqrt{\boldsymbol{b}^2+z^2}$, and the measured values for Pb are $\rho_0=0.1612$, $R=6.62$ fm, $a=0.545$ fm. For the proton density distribution, the Gaussian form is used

$$\rho_{\rm p}(\boldsymbol{b},z)=\frac{{\rm e}^{-r^2/(2B)}}{(2\pi B)^{3/2}}. \quad (8)$$

Because of gluon saturation, the inelastic nucleon-nucleon cross section $\sigma_{\rm in}$ should grow as $\sqrt{s}$ increases. This will result in a broadening of the nucleon density distribution in position space. Therefore, the Gaussian width B should be written as a function of $\sqrt{s}$ [4]

$$B(\sqrt{s})=\frac{\sigma_{\rm in}(\sqrt{s})}{14.30}{\rm fm}^2, \quad (9)$$

with $\sigma_{\rm in}(\sqrt{s})$=52, 60, 70.45, 72, 76.3 mb at $\sqrt{s}$=0.9, 2.36, 7, 8.8, 14 TeV, respectively [9, 14, 15].

In this paper, we also assume the gluon saturation scale should have a small dependence on $\sqrt{s}$ through the 3-dimensional rms radius of the proton [16]

$$Q_{\rm s,p(A)}^2(\sqrt{s})=Q_{\rm s,p(A)}^2(\sqrt{s_0})\left(\frac{\pi r_{\rm rms,0}^2}{\pi r_{\rm rms}^2}\right)^{1/\delta}, \quad (10)$$

where $\delta=0.8$ and the 3-dimensional rms radius $r_{\rm rms}=\sqrt{\langle r^2\rangle}=\sqrt{3B}$.

The single hadron distribution is obtained by convolving Eq. (1) with the fragmentation function for gluons into charged hadrons $D_{\rm g\to h}$

$$\frac{{\rm d}N_{\rm h}(\boldsymbol{b})}{{\rm d}^2\boldsymbol{p}_{\rm T}}=\int{\rm d}z\frac{{\rm d}N_{\rm g}(\boldsymbol{b})}{{\rm d}^2\boldsymbol{q}_{\rm T}}D_{\rm g\to h}(z,Q^2), \quad (11)$$

where $Q^2\approx p_{\rm T}^2$ and z is the fraction of the gluon energy carried by the baryon fragment. For the fragmentation function, we will use the Albino Kniehl Kramer (AKK08) [17] parameterizations.

3 Negative binomial distribution in the glasma flux tube picture

Negative binomial multiplicity distribution is an interesting and important feature observed in multiplicity distributions of charged hadron production in high energy collisions. In the glasma flux tube framework [11], the negative binomial distribution can be derived as

$$P_{\mathrm{n}}^{\mathrm{NBD}}(\bar{n},k)=\frac{\Gamma(k+n)}{\Gamma(k)\Gamma(n+1)}\left(\frac{\bar{n}}{k}\right)^{n}\left(1+\frac{\bar{n}}{k}\right)^{-n-k}, \quad (12)$$

where the parameter k and mean multiplicity $\bar{n}$ are all considered as functions of the impact parameter. The parameter k in the saturation approach is defined to be

$$k(\boldsymbol{b})=\zeta\frac{(N_{\mathrm{c}}^2-1)Q_{\mathrm{s,p}}^2S_{\perp}(\boldsymbol{b})}{2\pi}, \quad (13)$$

where ζ is a dimensionless parameter and $S_{\perp}$ is the overlap area of the two hadrons [11]. For a given impact parameter $\boldsymbol{b}$,

$$Q_{\mathrm{s,p}}^2S_{\perp}(\boldsymbol{b})=\int\mathrm{d}^2\boldsymbol{s}_{\perp}Q_{\mathrm{s,p}}^2(\boldsymbol{s}_{\perp},\boldsymbol{b}), \quad (14)$$

where $Q_{\mathrm{s,p}}$ in the overlap area of the two hadrons is chosen to be $Q_{\mathrm{s,p}}(\boldsymbol{s}_{\perp},\boldsymbol{b})=\min\{Q_{\mathrm{s,p}}(\boldsymbol{s}_{\perp}),Q_{\mathrm{s,p}}(\boldsymbol{s}_{\perp}-\boldsymbol{b})\}$. The mean multiplicity $\bar{n}$ can be obtained by integrating Eq. (11) over $\boldsymbol{p}_{\mathrm{T}}$

$$\bar{n}(\boldsymbol{b})=C_{\mathrm{m}}\int\mathrm{d}^2\boldsymbol{p}_{\mathrm{T}}\frac{\mathrm{d}N(\boldsymbol{b})}{\mathrm{d}^2\boldsymbol{p}_{\mathrm{T}}}, \quad (15)$$

where the pre-factor C_{m} is proportional to σ_{in}.

In order to compute the probability distribution as a function of multiplicity, one should convolve the NBD at a given impact parameter (Eq. (12)) with the probability for an inelastic collision $\left(\frac{\mathrm{d}P_{\mathrm{inel}}}{\mathrm{d}^2\boldsymbol{b}}\right)$ at the same impact parameter. Thus, the probability distribution for producing n particle can be given by

$$P(n)=\int\mathrm{d}^2\boldsymbol{b}\frac{\mathrm{d}P_{\mathrm{inel}}}{\mathrm{d}^2\boldsymbol{b}}P_{\mathrm{n}}^{\mathrm{NBD}}(\bar{n}(\boldsymbol{b}),k(\boldsymbol{b})), \quad (16)$$

where the probability distribution can be given in impact parameter eikonal models [18]

$$\frac{\mathrm{d}P_{\mathrm{inel}}}{\mathrm{d}^2\boldsymbol{b}}=\frac{1-\exp(-\sigma_{\mathrm{gg}}T_{\mathrm{pp}})}{\int\mathrm{d}^2\boldsymbol{b}[1-\exp(-\sigma_{\mathrm{gg}}T_{\mathrm{pp}})]}, \quad (17)$$

with the energy dependent quantity $\sigma_{\mathrm{gg}}=4\pi\lambda B$ [4]. The overlap function for two protons at a given impact parameter can be expressed as

$$T_{\mathrm{pp}}(\boldsymbol{b})=\int\mathrm{d}^2\boldsymbol{s}_{\perp}T_{\mathrm{p}}(\boldsymbol{s}_{\perp})T_{\mathrm{p}}(\boldsymbol{s}_{\perp}-\boldsymbol{b}). \quad (18)$$

4 Results and discussion

Charged hadron transverse momentum distributions in p+p collisions at different collision energies are shown in Fig. 1. The p_{T} distributions are averaged over the η range from -2.4 to 2.4. The rapidity (y) in Eq. (1) can be changed into the pseudo-rapidity (η) using the transformation

$$y(\eta)=\frac{1}{2}\ln\frac{\sqrt{\cosh^2\eta+m_0^2/p_{\mathrm{T}}^2}+\sinh\eta}{\sqrt{\cosh^2\eta+m_0^2/p_{\mathrm{T}}^2}-\sinh\eta}, \quad (19)$$

where $m_0(\sim\Lambda_{\mathrm{QCD}})$ is the rest mass of the particle. The experimental data come from CMS and ALICE [1, 2]. The parameter $\xi(=0.51)$ in Eq. (2) can be obtained by a χ^2 analysis with the experimental data [19, 20]. The solid curves are the results with the proton density distribution given in Eq. (8). For comparison, we also give the results (dashed curves) for the proton density distribution with a parameter-fixed dipole form [21], which was used in our previous work [22]. Fig. 1(a) shows the results with the KLN model. It is shown that the theoretical results with the modified Gaussian form are in good agreement with the experimental data. For the parameter-fixed dipole form, the theoretical results have a little deviation from the experimental data at small p_{T}. Fig. 1(b) shows the results with the KLR-AdS/CFT model. It is shown that the theoretical results fit the experimental data only at $\sqrt{s}$=7 TeV while p_{T} is small. The reason is that the KLR-AdS/CFT model is an effective model at small Bjorken-x ($x<10^{-4}$). At large p_{T} or small $\sqrt{s}$, $x_{1,2}(=p_{\mathrm{T}}/\sqrt{s}\cdot\exp(\pm y))$ is out of the valid range of this model.

In Fig. 2, we show the results for the average transverse momentum $\langle p_{\mathrm{T}}\rangle$ of charged particles versus the charged particle multiplicity N_{ch} in p+p collisions at $\sqrt{s}=$ 0.9, 2.76 and 7 TeV with the KLN model. The average transverse momentum at different energies can be expressed as [23]

$$\langle p_{\mathrm{T}}\rangle\propto\frac{B}{A}\sqrt{\frac{\mathrm{d}N_{\mathrm{g}}/\mathrm{d}\eta}{AS_{\perp}}}, \quad (20)$$

where $A=\int\frac{\mathrm{d}N_{\mathrm{g}}}{\mathrm{d}^2\boldsymbol{p}_{\mathrm{T}}}\mathrm{d}^2\boldsymbol{p}_{\mathrm{T}}/\bar{Q}_{\mathrm{s}}(\sqrt{s})$ and $B=\int p_{\mathrm{T}}\frac{\mathrm{d}N_{\mathrm{g}}}{\mathrm{d}^2\boldsymbol{p}_{\mathrm{T}}}\mathrm{d}^2\boldsymbol{p}_{\mathrm{T}}/\bar{Q}_{\mathrm{s}}^2(\sqrt{s})$ with $\bar{Q}_{\mathrm{s}}(\sqrt{s})=Q_0(\sqrt{s}/Q_0)^{\lambda/(2+\lambda)}$. The relation between $\mathrm{d}N_{\mathrm{g}}/\mathrm{d}\eta$ and N_{ch} is

$$N_{\mathrm{ch}}=\frac{1}{\Delta\eta}\int\frac{\mathrm{d}N_{\mathrm{g}}}{\mathrm{d}\eta}\mathrm{d}\eta.$$

The kinematic ranges for pseudo-rapidity and transverse momentum are $|\eta|<0.3$ and $0.15<p_{\mathrm{T}}<10$ GeV. Fig. 2(a) and (b) are the results with the Gaussian proton density distribution and the parameter-fixed dipole form distribution, respectively. The experimental data come from ALICE [24], and the theoretical results show good but not perfect agreement with the experimental data.

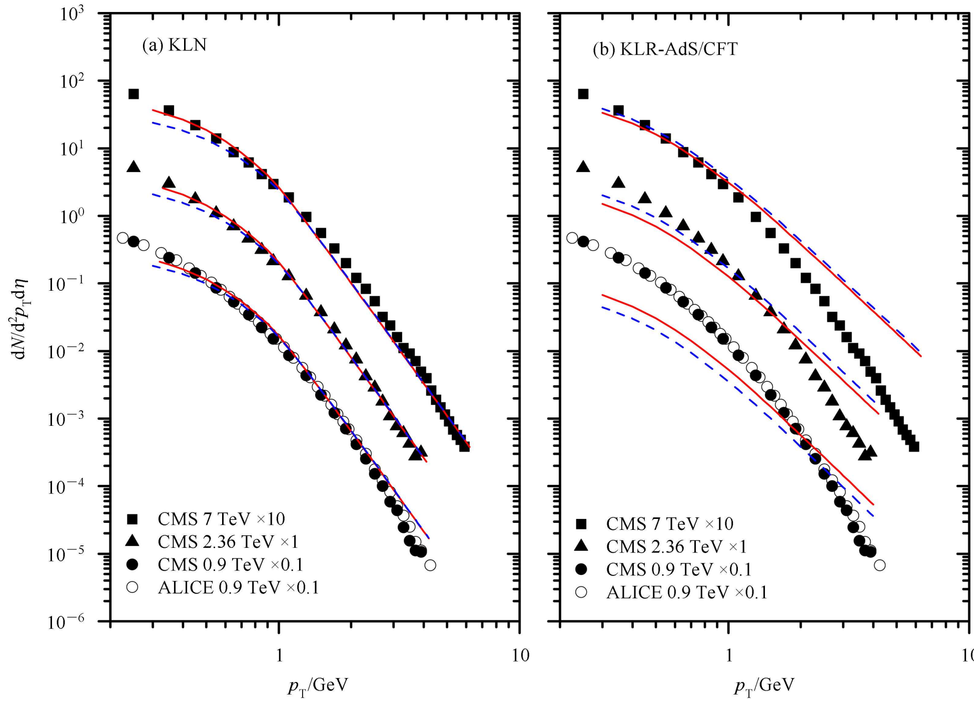

Fig. 1. (color online) Charged hadron p_T distributions for p+p collisions averaged over the range of $|\eta|<2.4$ with (a) the KLN model and (b) the KLR-AdS/CFT model. The solid and the dashed curves are the results with the modified Gaussian form and the parameter-fixed dipole form respectively for the proton density distribution. The experimental data come from CMS and ALICE [1, 2].

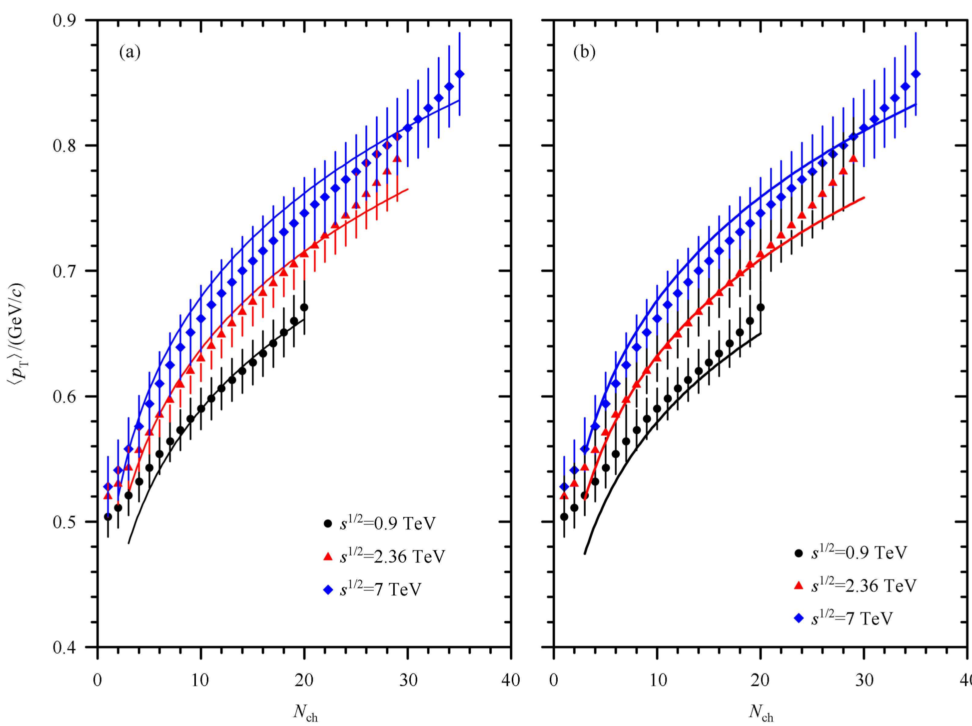

Fig. 2. (color online) Mean $\langle p_T\rangle$ in p+p collisions for three different LHC energies 0.9 TeV, 2.76 TeV and 7 TeV with the KLN model for (a) the modified Gaussian form and (b) the parameter-fixed dipole form for the proton density distribution. The data come from ALICE [24].

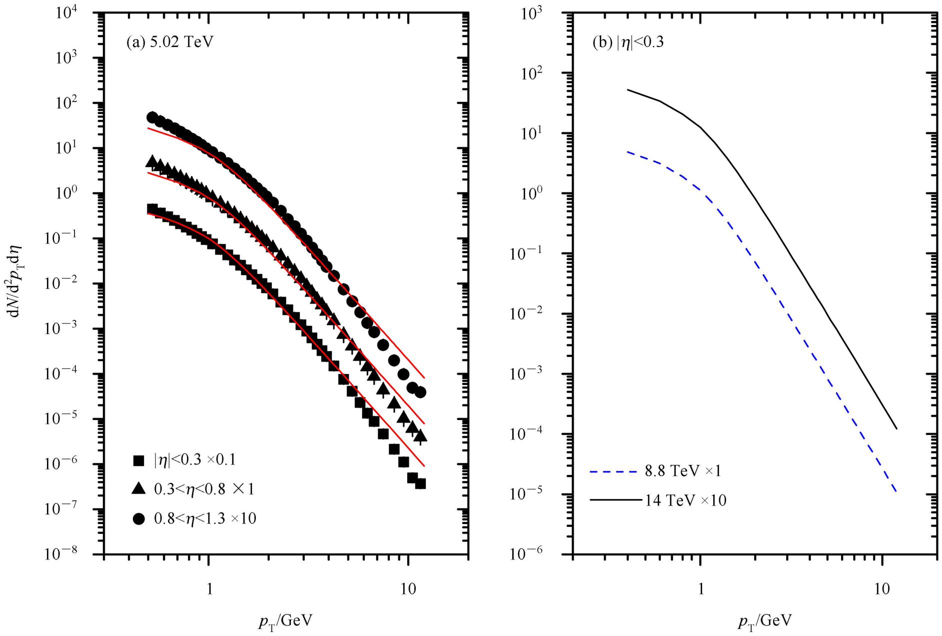

Fig. 3. (color online) Transverse momentum distributions of charged hadron in p+Pb collisions. (a) The results for different pseudo-rapidity ranges at $\sqrt{s}$=5.02 TeV. (b) The predicted results at $\sqrt{s}$=8.8 TeV and 14 TeV for pseudo-rapidity range $|\eta|$<0.3. The data come from ALICE [25].

In Fig. 3, the results with the KLN model for charged hadron $p_{\rm T}$ distributions in p+Pb (solid curves) collisions are given. Fig. 3(a) shows the results at $\sqrt{s}$=5.02 TeV for different pseudo-rapidity ranges $|\eta|<0.3$, $0.3<\eta<0.8$ and $0.8<\eta<1.3$. The experimental data come from ALICE [25]. In Fig. 3(b), the predicted results for $|\eta|<0.3$ at $\sqrt{s}$=8.8 TeV (dashed curve) and 14 TeV (solid curve) are also given. The theoretical results fit well with the experimental data at small $p_{\rm T}$ but show slight deviation at large $p_{\rm T}$.

Figure 4(a) shows the the probability distribution for an inelastic collision at b. The curves are the results at $\sqrt{s}=$ 0.9 TeV (solid curve), 2.36 TeV (dashed curve), 7 TeV (dash-dotted curve), and 14 TeV (dotted curve). The results show that the probability distributions $2\pi b dP_{\rm inel}/{\rm d}^2\boldsymbol{b}_\perp$ at certain $\sqrt{s}$ have a sharply peaked distribution and the impact parameter b of the peak grows with increasing collision energy $\sqrt{s}$. Fig. 4(b) shows the width parameter k versus impact parameter b. It is shown that the width parameter k becomes larger as $\sqrt{s}$ increases. This is because the number of flux tubes $Q_{\rm s}^2 S_\perp$ in k depends on the energy-dependent broadening thickness function $T_{\rm p}$.

The results for charged hadron multiplicity distributions in the range of $|\eta|<0.5$ and $|\eta|<1$ are shown in Fig. 5. The figures are the results at $\sqrt{s}=$ 0.9 TeV (a), 2.36 TeV (b), 7 TeV (c), and 14 TeV (d). The solid curves are the results with the glasma flux tube approach, and the dashed curves are the results without considering the nucleon's transverse position distribution. The data come from ALICE [26]. The parameter $\zeta=0.05$ is extracted from a fit to data at $\sqrt{s}=$ 2.36 TeV and used

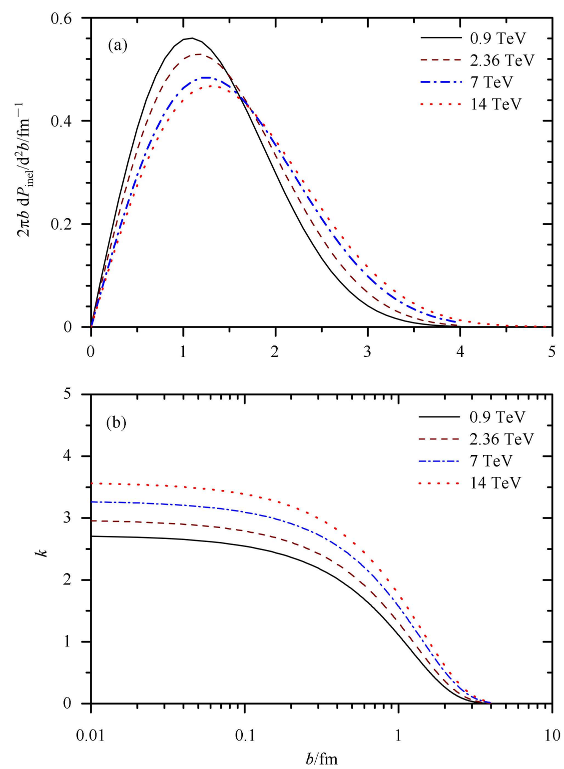

Fig. 4. (color online) The probability distribution for (a) inelastic collisions and (b) width parameter k as a function of impact parameter b.

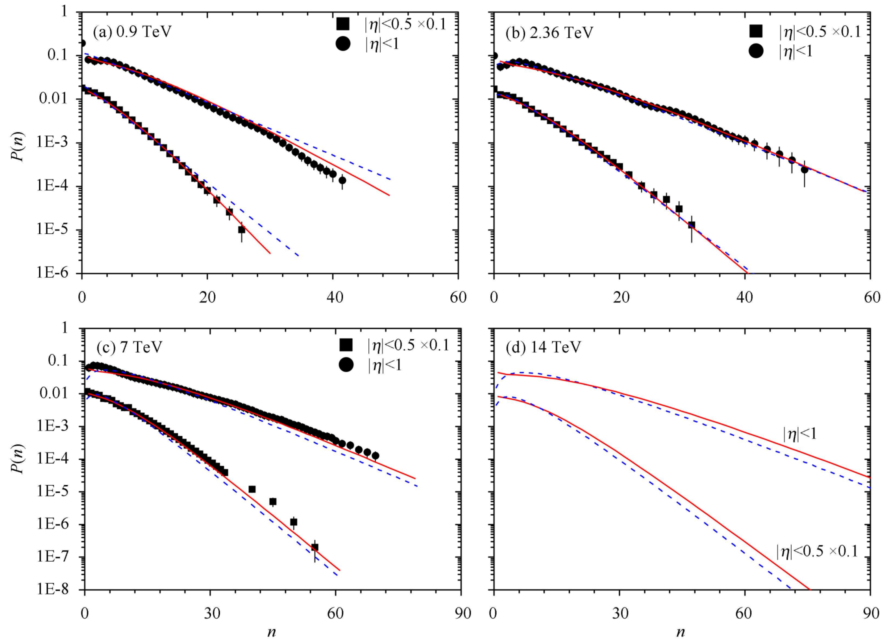

Fig. 5. (color online) Multiplicity distributions of charged hadrons in the range of $|\eta|<0.5$ and $|\eta|<1$. The figures are the results at $\sqrt{s}$=0.9 TeV (a) , 2.36 TeV (b), 7 TeV (c) and 14 TeV (d). The solid curves are the results with the glasma flux tube approach, and the dashed curves are the results without considering the nucleon's position distribution. The data come from ALICE [26].

for all other energies. It is shown that the theoretical results with the glasma flux tube approach are in good agreement with the experimental data at all collision energies. For the method without considering the transverse distribution, the theoretical results fit well to the data at $\sqrt{s}=$ 2.36 TeV but show deviations for other collisions at the highest multiplicities.

In summary, charged hadron $p_{\rm T}$ spectra in p+p and p+Pb collisions at various collision energies were studied with the CGC approach. By considering an energy-dependent broadening of the nucleon density distribution in position space, the theoretical results of the KLN model are in good agreement with the experimental data from CMS and ALICE. The probability distribution for producing n particles at different pseudo-rapidity ranges were also studied in the picture of glasma flux tube, and the results fit well with the experimental data. The predicted results for $p_{\rm T}$ and multiplicity distributions in p+p and p+Pb collisions will be examined in forthcoming experiments at the LHC.

References

1 CMS collaboration. Phys. Rev. Lett., 2010, **105**: 022002
2 ALICE collaboration. Phys. Lett. B, 2010, **688**: 21
3 Gelis F, Iancu E, Jalilian-Marian J et al. Ann. Rev. Nucl. Part. Sci., 2010, **60**: 463
4 Heinz U, Moreland J S. Phys. Rev. C, 2011, **84**: 054905
5 Golec-Biernat K, Wüsthoff M. Phys. Rev. D, 1999, **59**: 014017
6 Kharzeev D, Levin E, Nardi M. Nucl. Phys. A, 2004, **730**: 448
7 Iancu E, Itakura K, Munier S. Phys. Lett. B, 2004, **590**: 199
8 Kovchegov Y V, LU Z, Rezaeian A H. Phys. Rev. D, 2009, **80**: 074023
9 Dumitru A, Kharzeev D E, Levin E M et al. Phys. Rev. C, 2012, **85**: 044920
10 Premomoy G. Phys. Rev. D, 2012, **85**: 054017
11 Tribedy P, Venugopalan R. Nucl. Phys. A, 2011, **850**: 136
12 Kuhlman A, Heinz U, Kovchegov Y V. Phys. Lett. B, 2006, **638**: 171
13 deVries H, deJager C W, deVries C. At. Data Nucl. Data Tables, 1987, **36**: 495; Miller M L, Reygers K, Sanders S J et al. Ann. Rev. Nucl. Part. Sci., 2007, **57**: 205
14 Albacete J L, Dumitru A, Fujii H et al. Nucl. Phys. A, 2013, **897**: 1
15 Block M M, Halzen F. Phys. Rev. D, 2011, **83**: 077901
16 Armesto N, Salgado C A, Wiedemann U A. Phys. Rev. Lett., 2005, **94**: 022002
17 Albino S, Kniehl B A, Kramer G. Nucl. Phys. B, 2008, **803**: 42
18 d'Enterria D, Eyyubova G K, Korotkikh V L et al. Eur. Phys. J. C, 2010, **66**: 173
19 WANG H M, HOU Z Y, ZHANG B A et al. Int. J. Mod. Phys. A, 2010, **25**: 1009
20 WANG H M, HOU Z Y, SUN X J. Nucl. Sci. Tech., 2014, **25**: 040502
21 Frankfurt L, Strikman M, Weiss C. Phys. Rev. D, 2004, **69**: 114010
22 WANG H M, HOU Z Y, SUN X J. Chin. Phys. Lett., 2010, **27**: 052502
23 McLerran L, Praszalowicz M. hep-ph/1407.6687
24 ALICE collaboration. Phys. Lett. B, 2013, **727**: 371
25 ALICE collaboration. Phys. Rev. Lett., 2013, **110**: 082302
26 Aamodt K, Abel N, Abeysekara U et al. Eur. Phys. J. C, 2010, **68**: 345